JOURNAL OF MATERIALS SCIENCE 37 (2002) 5261 – 5266

Synthesis of high-ordered $LiNi_{0.5}Co_{0.5}O_2$ nanowire arrays by AAO template and its structural properties

YINGKE ZHOU, HULIN LI*
Chemistry Department of Lanzhou University, Lanzhou 730000, People's Republic of China
E-mail: lihl@lzu.edu.cn

High-ordered $LiNi_{0.5}Co_{0.5}O_2$ nanowire arrays were prepared using porous anodic aluminum oxide (AAO) template from sol-gel solution containing Li(OAc), $Ni(OAc)_2$ and $Co(OAc)_2$. Electron microscope results showed that uniform length and diameter of $LiNi_{0.5}Co_{0.5}O_2$ nanowires were obtained, and the length and diameter of $LiNi_{0.5}Co_{0.5}O_2$ nanowires are dependent on the pore diameter and the thickness of the applied AAO template. X-ray diffraction and electron diffraction pattern investigations demonstrate that $LiNi_{0.5}Co_{0.5}O_2$ nanowires are a layered structure of $LiNi_{0.5}Co_{0.5}O_2$ crystal. X-ray photoelectron spectroscopy analysis indicates that the most closely resemble stoichiometric layered $LiNi_{0.5}Co_{0.5}O_2$ material has been obtained.

1. Introduction

Lithium nickel-cobalt oxides, $LiNi_{1-y}Co_yO_2 (0 \leq y \leq 1)$ are solid solution of the layered end-compounds, namely $LiMO_2$ (M = Ni,Co). Thay are attracting materials for their technological use as cathodes of rechargeable lithium batteries because lithium ions are electrochemically extracted and inserted with high reversibility [1–12]. These compounds show higher operating voltages than the conventional 3-volt systems. They are also of interest due to several advantages in comparison with the parent end-members $LiCoO_2$ and $LiNiO_2$, i.e., structural and electrochemical [4]. Exhibiting a lower potential, $LiNi_{1-y}Co_yO_2$ oxides are less active for an organic electrolyte oxidation and prevent the nickel dioxide formation which occurs with an associated exothermic reaction.

The standard high-temperature (HT) $LiNi_{1-y}Co_yO_2$ powders have usually been prepared by the solid-state reaction in which hydroxides or carbonates are calcined at about 800–900°C for a prolonged period [13]. Research works in this area have focused the attention on new synthesis route for low-temperature crystallized oxides (LT-$LiMO_2$), which showed some promise in improving the cycle life of rechargeable lithium batteries [14–17]. Though research of $LiNi_{1-y}Co_yO_2$ has been enormous, high-ordered $LiNi_{1-y}Co_yO_2$ nanowire arrays haven't been reported. In recent years, nanostructured electrode materials have attracted great interests since the capacity of electrode material is critically affected by the morphology of the materials which contribute to different ways of diffusion processes of Li^+ ion [18]. The nano-structured materials have been explored for using as cathode and anode materials in lithium-ion battery in recent years. Novel nano-structured electrode material is not only a good model system for the research of intercalation reaction of Li^+, but also it is a promising material in some special Li-ion battery systems such as micro-batteries. As an important preparation method of nano-structured materials, template method [19] have successfully played crucial role in a variety of areas. Different kinds of template such as anodic porous alumina, polymer and nano-channel glass templates have been widely investigated. Normally anodized aluminum in appropriate acid solution forms anodic porous alumina template. Compared with other template, the size of holes of the template can be readily controlled by properly adjusting the condition of anodization [20]. In this paper, we firstly apply Sol-Gel-Template method to prepare $LiNi_{0.5}Co_{0.5}O_2$ as high-ordered nanowire arrays, which are distinctly different from the results of conventional methods.

Sol-gel chemistry has recently evolved as a powerful approach for preparing inorganic materials such as glasses and ceramics [21–23]. This method for the synthesis of inorganic materials has a number of advantages over more conventional synthetic procedures. For example, high-purity materials can be synthesized at a lower temperature. In addition, homogeneous multicomponent systems can be obtained by mixing precursor solutions. This allows for easy chemical doping of the materials prepared. Finally, the rheological properties of the sol and the gel can be utilized in processing the material, for example, by dip coating of thin films, spinning of fibers, etc. [23, 24]. Here we have combined the concepts of Sol-Gel synthesis and template

*Author to whom all correspondence should be addressed.

preparation of nanomaterials to yield a new general route for preparing $LiNi_{0.5}Co_{0.5}O_2$ nanoarrays. This was accomplished by conducting Sol-Gel synthesis within the pores of various nanoporous membranes, and monodisperse nanoarrays of $LiNi_{0.5}Co_{0.5}O_2$ nanowires are obtained.

2. Experimental

2.1. Membrane preparation

High-purity aluminum sheets (99.99%, 20 mm × 10 mm) were employed in our experiment. Prior to anodization, the metal surfaces were degreased, etched in alkaline solution and rinsed in distilled water, then electropolished to achieve a smooth surface. It was necessary to immerse the samples in concentrated acid or alkaline solution for several minutes to remove the oxide layer formed during the electropolishing process. All samples were rinsed in distilled water and then transferred to a nitrogen environment. The resultant clean aluminum samples were anodized at constant potential in phosphic acid (99–101 V, 0°C, Pt sheet as a counter electrode). Then the whole sheet was put into saturated $HgCl_2$ solution to separate template membrane with the Al substrate. The membrane was rinsed with distilled water and then immersed in 5% H_3PO_4 solution for about 30 min at 30°C in order to dissolve the barrier-type part on the bottom of nano-holes. AAO templates were characterized by using transmission electron microscopy (TEM) and scanning electron microscopy (SEM).

2.2. Preparation of $LiNi_{0.5}Co_{0.5}O_2$ nanowire arrays

Metal acetates were used as the cationic sources, and citric acid and ethylene glycol as the monomers for forming the polymeric matrix. 1 : 1 : 2 molar ratio $Ni(OAc)_2$, $Co(OAc)_2$ and LiOAc were dissolved in a mixture of citric acid and ethylene glycol (1 : 4, molar ratio). A clear solution was then produced, and it was heated at 140°C to induced esterification and distilled out excess ethylene glycol. Thus the sol is obtained.

The alumina template membrane is dipped into the sol for the desired amount of time, removed, and the excess sol on the membrane surface was wiped off using a laboratory tissue, followed by drying under vacuum at 50°C for 1 h. The membrane surface was carefully wiped again to remove salts crystallized on the surface and heated at 600°C for 10 hours in open air, resulting in formation of arrays of $LiNi_{0.5}Co_{0.5}O_2$ nano-wires in the inside of the pores of the AAO template.

2.3. Characterization of $LiNi_{0.5}Co_{0.5}O_2$ nanowire arrays

The structure and morphology properties of $LiNi_{0.5}Co_{0.5}O_2$ nanowire arrays were characterized by several techniques. X-ray diffraction (XRD) data of the template membrane were collected using a Rigaku D/MAX2400 diffractometer with Cu K_α radiation. The TEM (Hitachi 600, Japan) was used to observe the morphology and degree of agglomeration. Before TEM observation the alumina template membrane was dissolved by using 3 M NaOH, and then diluted with distilled water for three times. Scanning electron microscopic (SEM) images were recorded with JSM-5600LV microscope. For SEM sample, the alumina template membrane was attached on a Cu cylinder. Then, 2 drops of 3 M NaOH were dropped on the sample to dissolve partial membrane, and then the samples were sputter-coated with gold before the SEM measurement in order to increase their conductivity. The X-ray Photoelectron Spectroscopy (XPS) data were obtained by a V. G. ESCA Lab. 2201-XL photoelectron spectrometer with Mg K_α source, a concentric hemispherical analyzer operating in fixed analyzer transmission mode and a multi-channel detector, the pressure in analysis chamber is less than 2×10^{-10} Torr. The spectra were acquired with 50 eV pass energy and 1 mm^2 spot (large area mode without using XL lens). The binding energy was calibrated with reference to the C 1s level of carbon (285.0 eV).

3. Results and discussion

3.1. TEM and SEM analysis

When anodized in an acidic electrolyte, aluminum forms a porous oxide with very uniform and parallel pores open at one end and sealed at the other [25–27]. Its structure is described as a close-packed array of columnar cells, each containing a central pore of which the side and interval can be controlled by changing the forming conditions [25–27]. Fig. 1a presents the TEM

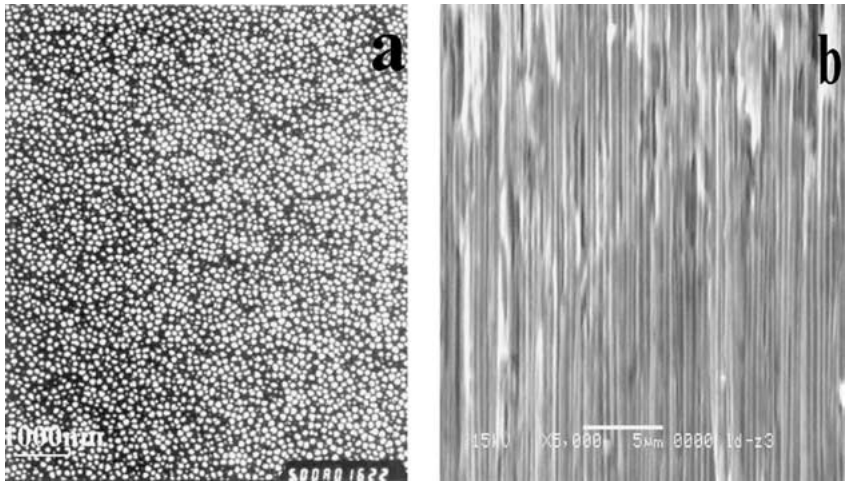

Figure 1 TEM photograph of AAO template (a) and SEM photograph of AAO template (b).

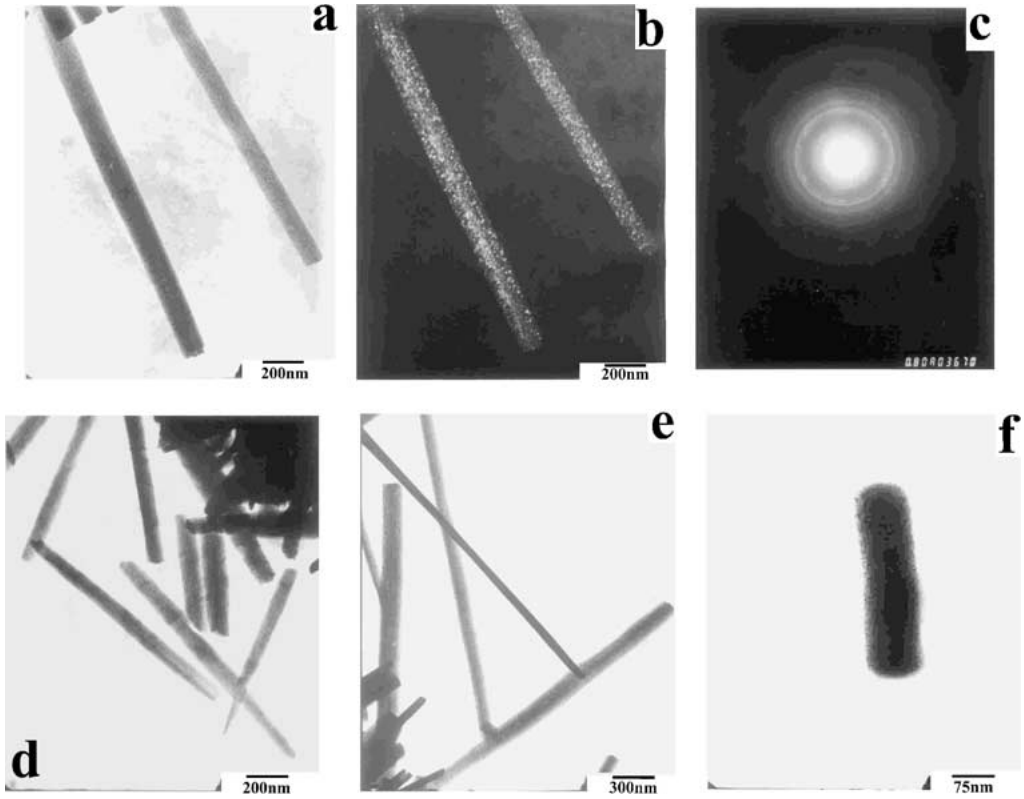

Figure 2 TEM photographs of $LiNi_{0.5}Co_{0.5}O_2$ nanometer wires: (a–c) The bright field TEM image, dark field TEM image and corresponding electron diffraction pattern; (d, e) TEM image of several $LiNi_{0.5}Co_{0.5}O_2$ nanowires; (f) TEM image of a single $LiNi_{0.5}Co_{0.5}O_2$ nanowire.

photograph of porous AAO template with a pore diameter $d = 100 \pm 5$ nm, and a pore density of about 10^{11}–10^{12} cm^{-2}. Perfect hexagonal pore arrays can be observed within domains of microsize, which are separated from neighboring aluminum oxide domains with a different orientation of the pore lattice by grain boundaries. Thus, a poly-crystalline pore structure is observed. As the further observation, the SEM photograph is obtained in Fig. 1b, which depicts the cross-section of the AAO template with pores parallel to each other and perpendicular to the surface of the membrane.

The TEM images of $LiNi_{0.5}Co_{0.5}O_2$ nanowires formed by AAO template are shown in Fig. 2. The as-produced nanowires are uniformly distributed and have a diameter of around 100 nm. The length and the diameter of these nanowires correspond exactly to that of the templates. Fig. 2a, and b showed TEM images of two parallel $LiNi_{0.5}Co_{0.5}O_2$ nanowires at light and dark field, respectively. We can see these images are of the same two $LiNi_{0.5}Co_{0.5}O_2$ nanowires. There are many bright little dots in the nanowires of Fig. 2b, which indicates that $LiNi_{0.5}Co_{0.5}O_2$ nanowire consists of a lot of little crystals, and these bright crystals exactly diffracted out from this angle when this image is taken. Here we can conclude that the $LiNi_{0.5}Co_{0.5}O_2$ nanowire obtained in our experiment is polycrystalline. The corresponding electron diffraction pattern taken from this $LiNi_{0.5}Co_{0.5}O_2$ nanowire is shown in Fig. 2c. The diffraction spots correspond to the (003), (101), (104) and (110) diffraction planes of layered $LiNi_{0.5}Co_{0.5}O_2$ crystalline according to the electron diffraction formula. Fig. 2d shows major ten $LiNi_{0.5}Co_{0.5}O_2$ nanowires, in which four nanowires are observed only one end, and the other ends of the four seem to adhere to each other. The reason is that the aluminum matrix is not dissolved completely and the residual makes so. Fig. 2d shows major four $LiNi_{0.5}Co_{0.5}O_2$ nanowires, of which three across with each other and form a triangle. The other one is separated from the three but overlapped by another nanowires ends. This image also shows these nanowires have uniform length and diameter, which corresponding pores of the employed AAO template. These nanowires are uniform distributed, which indicated the alumina matrix is dissolved completely. Fig. 2d shows another image of one $LiNi_{0.5}Co_{0.5}O_2$ nanowire.

Fig. 3 showed SEM images of $LiNi_{0.5}Co_{0.5}O_2$ nanowires grown by AAO template. These photographs show the nanowires are parallel to each other, and few microscopic defects are found in these wires. Fig. 3a is cross-section of the $LiNi_{0.5}Co_{0.5}O_2$ nanowire arrays and Fig. 3b is the magnified local image of the cross-section, and we can see the whole cross-section from two plane of which, namely, the stereo-structure of the nanowire arrays is clearly obtained. These photographs show that nanowires are parallel to each other, uniformly distributed, high ordered and few microscopic defects are found in these wires. This is because the alumina matrix is only partial dissolved, which makes the nanowires keep the situations within the pores of the nanoporous alumina matrix. Fig. 3c is the magnified local image of the top surface of $LiNi_{0.5}Co_{0.5}O_2$ nanowire arrays. Fig. 3d presents a cluster of $LiNi_{0.5}Co_{0.5}O_2$ nanowires, of which the alumina matrix is almost dissolved completely, and only the bottom adhere together due to the residual alumina, and which make the nanowires diverge from the bottom

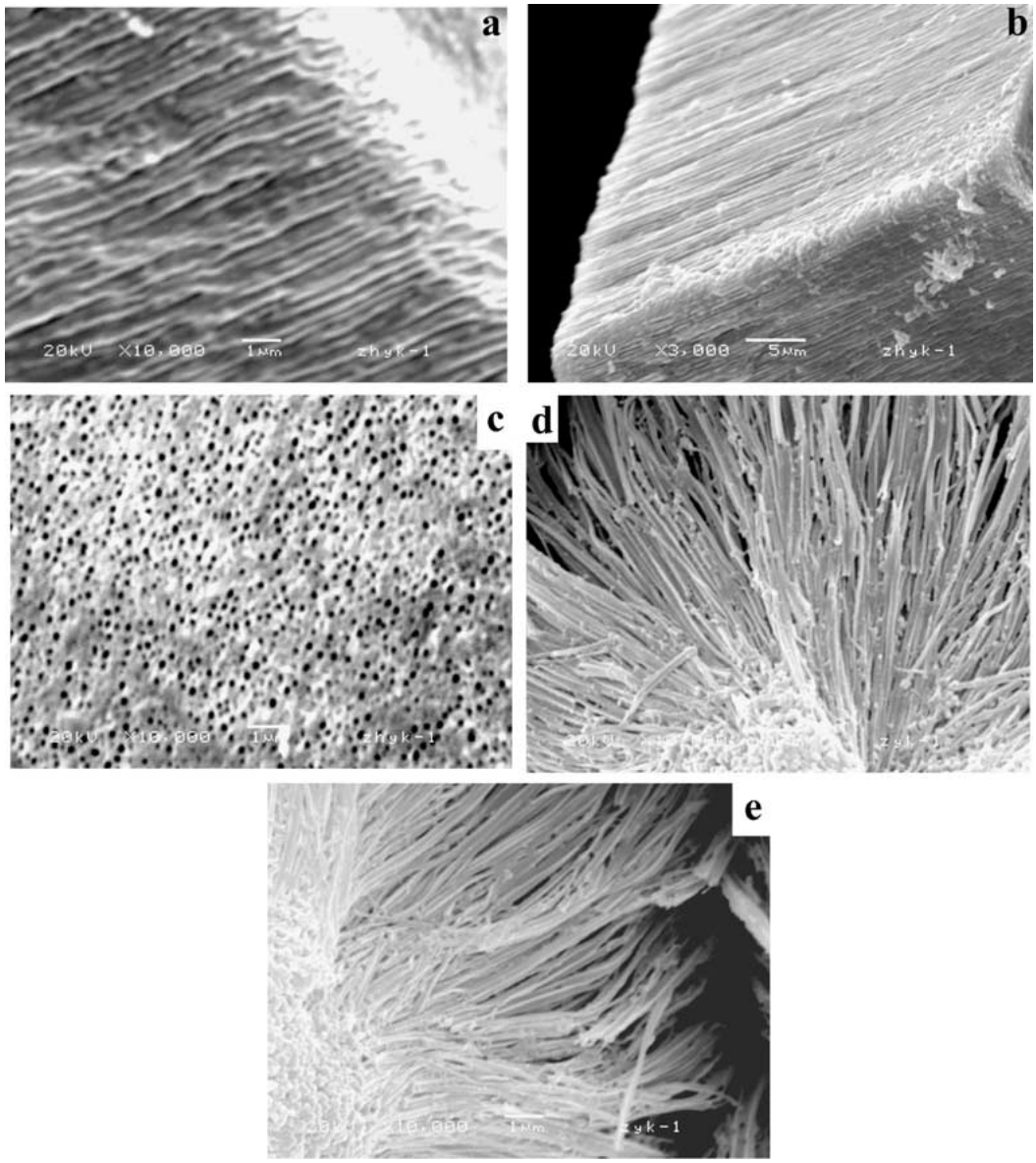

Figure 3 SEM photographs of $LiNi_{0.5}Co_{0.5}O_2$ nanowire arrays: (a) cross-section of $LiNi_{0.5}Co_{0.5}O_2$ nanowire arrays; (b) magnified local image of the cross-section of $LiNi_{0.5}Co_{0.5}O_2$ nanowires; (c) the top surface of $LiNi_{0.5}Co_{0.5}O_2$ nanowire arrays; (d) a cluster of $LiNi_{0.5}Co_{0.5}O_2$ nanowires like a sector; (e) another clusters of $LiNi_{0.5}Co_{0.5}O_2$ nanowires.

like a sector. Fig. 3e is another cluster of $LiNi_{0.5}Co_{0.5}O_2$ nanowires similar to Fig. 3d. But in Fig. 3e, these nanowires form a fiber-brush and we can also see the uniformly distributed and ordered characteristic of a nanowires array from it. As a result, the lengths of $LiNi_{0.5}Co_{0.5}O_2$ nanowires are equivalent to the thickness of the applied template, and at the same time the outside diameter of these wires are equivalent to the pore diameter of the template membrane (100 nm).

3.2. XRD analysis

The ideal layered $LiNi_{0.5}Co_{0.5}O_2$ has a rock salt structure with lithium and transition metal cations occupying alternative layers of octahedral sites (3a and 3b sites, respectively) in a distorted cubic close-packed oxygen ion lattice (6c site) [28–30]. The XRD spectrum of $LiNi_{0.5}Co_{0.5}O_2$ nanowire arrays (within the AAO template) is shown in Fig. 4. Although the background diffraction peaks of Al_2O_3 template is very large, the major diffraction peaks of $LiNi_{0.5}Co_{0.5}O_2$ are observed, and which are closely corresponding to

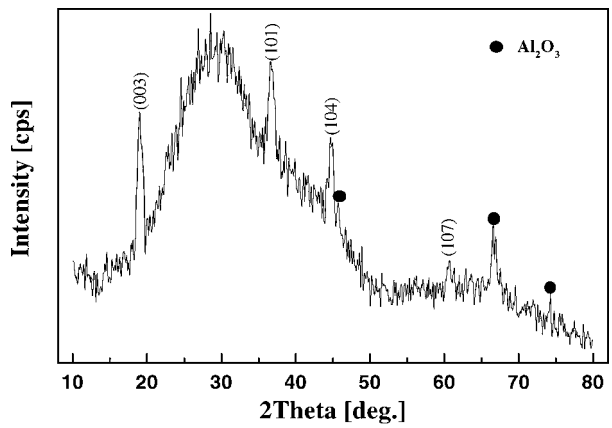

Figure 4 XRD patterns of $LiNi_{0.5}Co_{0.5}O_2$/alumina composite membrane.

layered $LiNi_{0.5}Co_{0.5}O_2$ (003), (101) and (104) plane. We can also see that all the diffraction peaks intensity of $LiNi_{0.5}Co_{0.5}O_2$ is smaller than that of Al_2O_3. The reason for weaker diffraction peaks of $LiNi_{0.5}Co_{0.5}O_2$

derived from a little quantity of $LiNi_{0.5}Co_{0.5}O_2$ in template and $LiNi_{0.5}Co_{0.5}O_2$ were not covered on the surface of template.

3.3. XPS analysis

The chemical composition of layered $LiNi_{0.5}Co_{0.5}O_2$ nanowire arrays (within the AAO template) was obtained by XPS measurements. In an X-ray photoelectron spectroscopy (XPS) experiment, the samples are exposed to monochromic X-radiation and the properties of inner-shell electrons are to be probed. The quantitative analysis of the $LiNi_{0.5}Co_{0.5}O_2$ is made from the integrated intensities of the Co 2p, Ni 2p and Li 1s lines, which are observed with the peaks attributed to oxygen in the XPS spectrum. Of course, the peaks corresponding to aluminium is also recorded in the spectrum. Fig. 5 (a–e) displays the XPS spectra of Co 2p, Ni 2p, Li 1s, O 1s and Al 2p core levels, respectively, for $LiNi_{0.5}Co_{0.5}O_2$/AAO composite. The line of Li 1s core level has a low intensity with a binding energy located at 54.4 eV (Fig. 5c). The line shape of the core levels O 1s and Al 2p are Gaussian-like with a binding energy of 530.2 eV (Fig. 5d) and 74.1 eV (Fig. 5e), respectively. We can see the peak intensity of O 1s and Al 2p are larger than the other elements, and this is in accord with the XRD analysis. And for the quantitative analysis of O, we used the area under the O 1s, but of which, the part that corresponding Al_2O_3 should be subtracted. The peaks located at 779.5 eV and 795.2 eV (Fig. 5b) are attributed to the spin-orbit splitting of the Co (2p) components, Co ($2p_{3/2}$) and Co ($2p_{1/2}$), respectively. The entire 2p region has to be included for quantitative analysis, because the total amount of the respective ion species is equal to the integral number over all Co (2p) states. Peaks of the Co 2p are close to previous reported [31], and we think that the Co ion is in a trivalent Co^{3+} low-spin state. Spectrum of Ni 2p corresponds to a divalent Ni^{2+} high-spin state, and this spectrum is quite similar to that of $LiNiO_2$, which

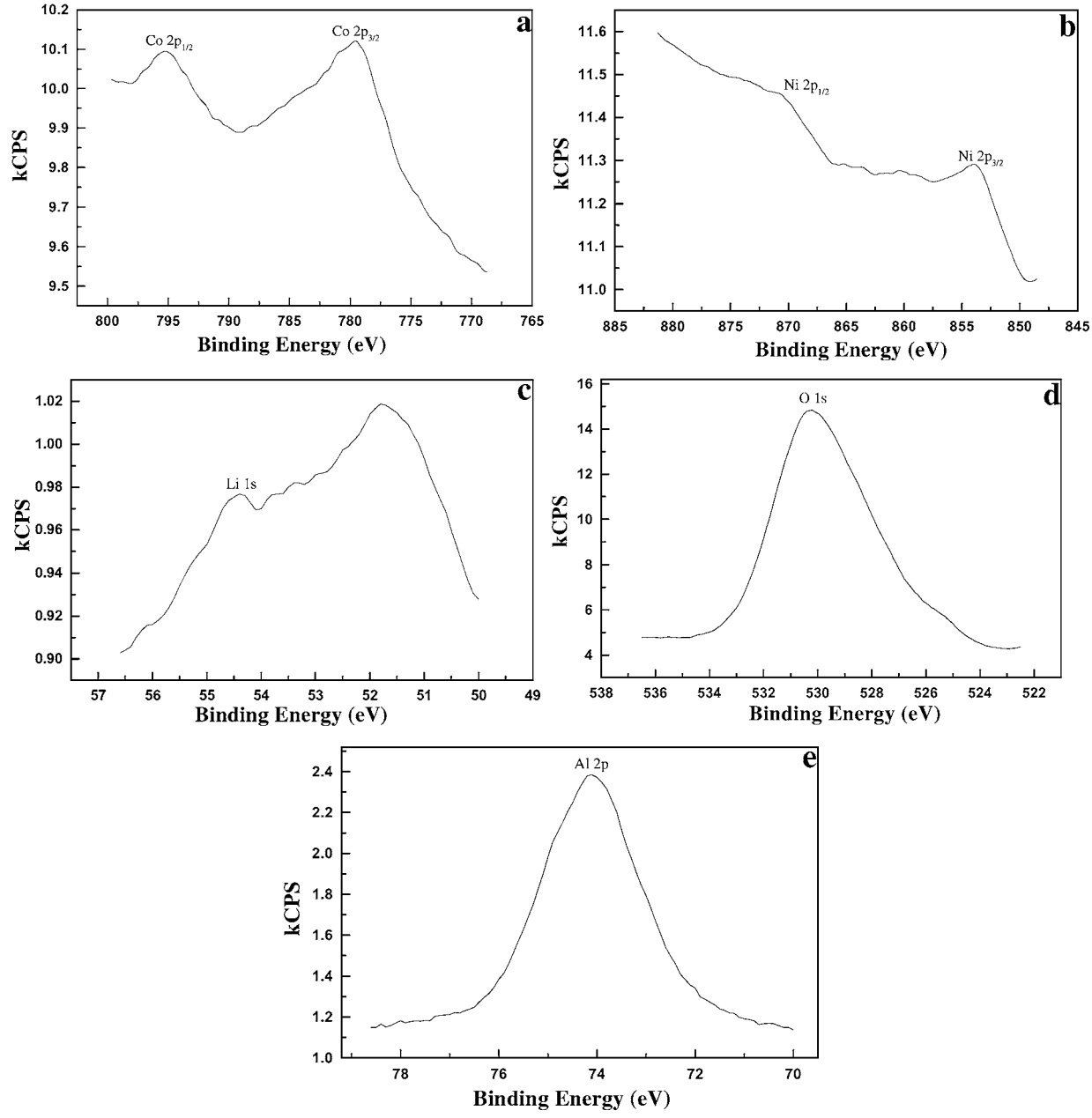

Figure 5 XPS spectra of (a) Co 2p; (b) Ni 2p; (c) Li 1s; (d) O 1s and (e) Al 2p core levels for $LiNi_{0.5}Co_{0.5}O_2$/alumina composite membrane.

also has Ni ion in a divalent Ni^{2+} high-spin state [32]. The missing charge at the Ni site in these compounds is compensated by a less negative oxygen ion, and this was confirmed by the analysis of O 1s XAS spectra of $Li_xNi_{1-x}O$ [33]. The intensity ratio between XPS peaks Ni 2p, Co 2p, Li 1s and O1s (after subtracted) shows that the $LiNi_{0.5}Co_{0.5}O_2$ product has been synthesized and most closely resemble stoichiometric layered material.

4. Conclusion

$LiNi_{0.5}Co_{0.5}O_2$ nanowire arrays were successfully fabricated by Sol-Gel template process. Investigations of X-ray diffraction and electron diffraction pattern demonstrated that $LiNi_{0.5}Co_{0.5}O_2$ nanowires are a layered structure of $LiNi_{0.5}Co_{0.5}O_2$ crystal. Electron microscope results show that these $LiNi_{0.5}Co_{0.5}O_2$ nanowires have a uniform length and diameter, and form a high-ordered array, and this is determined by the pore diameter and the thickness of the applied AAO template. XPS analysis indicates that most closely resemble stoichiometric layered material.

Acknowledgements

This work is supported by Nation Natural Science Foundation of China (No. 69871013). We would like to express our sincere thanks to Chief Engineer Gui-Xun Cao of Gansu Instrumental Analysis & Research Center for TEM measurement and analysis, to Chief Engineer Da-Kang Song of Material Department of Lanzhou University for measurement and analysis of XRD data.

References

1. T. OHZUKU, "Lithium Batteries, New Materials, Developments and Perspectives" (Elsevier, Amsterdam, 1993) p. 239.
2. R. J. GUMMOW and M. M. THACKERAY, *Solid State Ionics* **53–56** (1992) 681.
3. C. DELMAS and I. SAADOUNE, *ibid.* **53–56** (1992) 370.
4. T. OHZUKU, A. UEDA, M. NAGAYAMA, Y. IWAKOSHI and H. KOMORI, *Electrochim. Acta.* **38** (1993) 1159.
5. E. ZHECHEVA and R. STOYANOVA, *ibid.* **66** (1993) 143.
6. C. DELMAS, I. SAADOUNE and A. ROUGIER, *J. Power. Sources* **43/44** (1993) 595.
7. R. J. GOMMOW and M. M. THACKERAY, *J. Electrochem. Soc.* **140** (1993) 3365.
8. A. UEDA and T. OHZUKU, *ibid.* **141** (1994) 2010.
9. A. ROUGIER, I. SAADOUNE, P. GRAVEREAU, P. WILLMANN and C. DELMAS, *Solid State Ionics* **90** (1996) 83.
10. I. SAADOUNE and C. DELMAS, *J. Mater. Chem.* **6** (1996) 93.
11. Y. M. CHOI, S. I. PYUN and S. I. MOON, *Solid State Ionics* **89** (1996) 43.
12. I. SAADOUNE, M. MENETRIER and C. DELMAS, *J. Mater. Chem.* **7** (1997) 2505.
13. J. N. REIMERS and J. R. DAHN, *J. Electrochem. Soc.* **139** (1992) 2091.
14. P. BARBOUX, J. M. TARASCON and F. K. SHOKOOHI, *J. Solid State Chem.* **94** (1991) 185.
15. E. ROSSEN, J. N. REIMERS and J. R. DAHN, *Solid State Ionics* **62** (1993) 53.
16. B. GARCIA, P. BARBOUX, F. RIBOT, A. KAHN-HARARI, L. MAZEROLLES and N. BAFFIER, *ibid.* **80** (1995) 111.
17. I.-H. OH, S.-A. HONG and Y.-K. SUN, *J. Mater. Sci.* **32** (1997) 3177.
18. G. L. CHE, B. B. LAKSHMI, E. R. FISHER and C. R. MARTIN, *Nature* **393** (1998) 683.
19. F. SCHLOTTIF, M. TEXTOR, U. GERRGI and F. ROEWER, *J. Mater. Sci. Lett.* **18** (1999) 599.
20. U. GÖSELE, A. P. LI, K. NIELSCH, F. MULLER, W. ERFURTH and R. B. WSHRSPOHN, Extended Abstract 196th ECS Meeting, No. 158, Toronto, Canada, May, 2000.
21. C. J. BRINKER and G. W. SCHERER, "Sol-Gel Science" (Academic Press, New York, 1990).
22. L. L. HENCH and J. K. WEST, *Chem. Rev.* (Washington, D.C.) **90** (1990) 33.
23. M. A. AEGERTER, R. C. MEHROTA, I. OEHME, R. REISFELD, S. SAKKA, O. WOLFBERS and C. K. ORGENSEN, "Optical and Electronic Phenomena in Sol-Gel Glasses and Modern Applications," Vol. 85 (Springer-Verlag, Berlin, 1996).
24. B. B. LAKSHMI, C. J. PATRISSI and C. R. MARTIN, *Chem. Mater.* **9** (1997) 2544.
25. A. HUBER, T. E. HUBER, M. SADOQI, J. A. LUBIN, S. MANALIS and C. B. PRATER, *Science* **263** (1994) 800.
26. Y. PENG, H. L. ZHANG, S. L. PAN and H. L. LI, *J. Appl. Phys.* **87** (2000) 7405.
27. S. L. PAN, H. L. ZHANG, Y. PENG, Z. WANG and H. L. LI, *Chem. J. Chin. Univ.* **20** (1999) 1622.
28. C. DEIMAS and I. SAADOUNE, *Solid State Ionics* **53–56** (1992) 370.
29. A. UEDA and T. OHZUKU, *ibid.* **141** (1994) 2010.
30. T. OHZUKU, A. UEDA, M. NAGAYAMA, Y. IWAOSHI and H. KOMORY, *Electrochim. Acta.* **38** (1993) 1159.
31. L. A. MONTORO, M. ABBATE and J. M. ROSOLEN, *J. Electrochem. Soc.* **147** (2000) 1651.
32. M. ABBATE, F. M. F. DE GROOT, J. C. FUGGLE, A. FUJIMORE, Y. TOKURA, Y. FUJISHIMA, O. STREBEL, M. DOMKE, G. KAINDL, J. VAN ELP, B. T. THOLE, G. A. SAWATZKY, M. SACCHI and N. TSUDA, *Phys. Rev.* B **44** (1991) 5419.
33. P. KUIPER, G. KRUIZINGA, J. GHIJSEN, G. A. SAWATZKY and H. VERWEIJ, *Phys. Rev. Lett.* **62** (1989) 221.

Received 26 September 2001
and accepted 30 January 2002